Gyrator transform: properties and applications

José A. Rodrigo, Tatiana Alieva, María L. Calvo

Universidad Complutense de Madrid, Facultad de Ciencias Fsicas,Ciudad Universitaria s/n, Madrid 28040, Spain.

jarmar@fis.ucm.es

Abstract: In this work we formulate the main properties of the gyrator operation which produces a rotation in the twisting (position - spatial frequency) phase planes. This transform can be easily performed in paraxial optics that underlines its possible application for image processing, holography, beam characterization, mode conversion and quantum information. As an example, it is demonstrated the application of gyrator transform for the generation of a variety of stable modes.

References and links

1. H. M. Ozaktas, Z. Zalevsky, and M. Alper Kutay, The Fractional Fourier Transform with Applications in Optics and Signal Processing, John Wiley&Sons, NY, USA (2001).
2. M. W. Beijersbergen, L. Allen, H. E. L. O. Van der Veen and J. P. Woerdman, "Astigmatic laser mode converters and transfer of orbital angular momentum," Opt. Commun. **96**, 123-132 (1993).
3. E. G. Abramochkin and V. G. Volostnikov, "Beam transformations and nontransformed beams," Opt. Commun. **83**, 123-135 (1991).
4. E. G. Abramochkin and V. G. Volostnikov, "Generalized Gaussian beams," J. Opt. A.: Pure Appl. Opt. **6**, S157-S161 (2004).
5. G. F. Calvo, "Wigner representation and geometric transformations of optical orbital angular momentum spatial modes," Opt. Lett. **30**, 1207-1209 (2005).
6. R. Simon and K. B. Wolf , "Structure of the set of paraxial optical systems," J. Opt. Soc. Am. A **17**, 342-355 (2000).
7. K. B. Wolf, Geometric Optics on Phase Space, Springer-Verlag, Berlin (2004).
8. J. A. Rodrigo, T. Alieva, M. L. Calvo, "Optical system design for ortho-symplectic transformations in phase space," J. Opt. Soc. Am. A **23**, 2494-2500 (2006).
9. T. Alieva, V. Lopez, F. Agullo Lopez, L. B. Almeida, "The fractional Fourier transform in optical propagation problems, " J. Mod. Opt. **41**, 1037-1044 (1994).
10. M. Bastiaans and T. Alieva, "First-order optical systems with unimodular eigenvalues," J. Opt. Soc. Am. A **23**, 1875-1883 (2006).
11. T. Alieva and M. Bastiaans, "Mode mapping in paraxial lossless optics," Opt. Lett. **30**, 1461-1463 (2005).
12. M. Abramowitz and I. A. Stegun, eds., Pocketbook of Mathematical Functions, Frankfurt am Main, Germany (1984).
13. I. S. Gradshteyn and I.M. Ryzhik, Table of integrals, series and products, Academic Press, NY, USA (1996).
14. V. V. Kotlyar, S. N. Khonina, A. A. Almazov, V. A. Soifer, K. Jefimovs and J. Turunen, "Elliptic Laguerre–Gaussian beams," J. Opt. Soc. Am. A **23**, 43-56, (2006).

1. Introduction

Many interesting applications of the first-order optical systems for information processing have been proposed in the past decade. Some particular first-order optical systems, performing fractional Fourier transform, are used for shift-variant filtering, noise reduction, encryption [1].
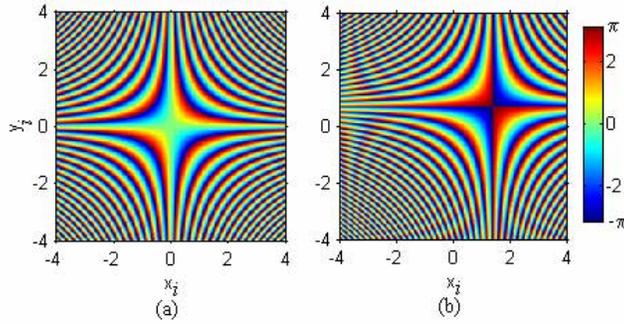
Fig. 1. Graphical representation for the phase structure associated to the gyrator kernel for $\alpha = \pi/4$, $x_o = y_o = 0$ (a) and $2x_o = y_o = 1$ (b). These figures (a) and (b) correspond to the exponential argument of the kernel.

Another ones serve as mode converters which permit to obtain the helicoidal vortex Laguerre-Gaussian (LG) mode after the propagation of the Hermite-Gaussian (HG) beam through these systems [2, 3, 4]. Besides LG modes, other stable modes carrying the fractional topological charge [4, 5] can be obtained by generalized mode converter which can be described by the gyrator transform (called in [6, 7] as a cross-gyrator). The gyrator transform as well as the fractional Fourier transform belong to the class of the linear canonical integral transforms. But in the contrast to the fractional Fourier transform (see for example [1] and references there in), the gyrator operation is still little known for the optical community. The purpose of this paper is to establish the main properties of the gyrator transform that opens the perspective of its application for optical information processing together with fractional Fourier transform. Including the gyrator transform in the list of image processing tools we enlarge a number of phase space domains for more appropriate image representation, filtering operation, holographic recording etc. As an example of gyrator action we demonstrate its application as a generator of stable modes living on the main meridian of the Poincaré spheres [5].

Gyrator operation is mathematically defined as a linear canonical integral transform which produces the rotation in position$-$spatial frequency planes (x, q_y) and (y, q_x) [6, 7] of phase space. Thus the gyrator transform (GT) at parameter α, which will be called below as a rotation angle, of a two-dimensional function $f_i(\mathbf{r}_i)$, associated in first order optics with complex field amplitude, can be written in the following form

$$f_o(\mathbf{r}_o) = R^\alpha[f_i(\mathbf{r}_i)](\mathbf{r}_o) = \iint f_i(x_i, y_i) K_\alpha(x_i, y_i, x_o, y_o) \, dx_i dy_i$$

$$= \frac{1}{|\sin\alpha|} \iint f_i(x_i, y_i) \exp\left(i2\pi \frac{(x_o y_o + x_i y_i)\cos\alpha - (x_i y_o + x_o y_i)}{\sin\alpha} \right) dx_i dy_i, \quad (1)$$

where $\mathbf{r}_{i,o}^t = (x_{i,o}, y_{i,o})$ indicates the input and output coordinates, respectively. Notice that t stands for transposition operation. For $\alpha = 0$ it corresponds to the identity transform, for $\alpha = \pi/2$ it reduces to the Fourier transform with rotation of the coordinates at $\pi/2$, for $\alpha = \pi$ the reverse transform described by the kernel $\delta(\mathbf{r}_o + \mathbf{r}_i)$ is obtained, meanwhile for $\alpha = 3\pi/2$ it corresponds to the inverse Fourier transform with rotation of the coordinates at $\pi/2$. For other angles α the kernel of the GT $K_\alpha(x_i, y_i, x_o, y_o)$ has a constant amplitude and a hyperbolic phase structure, which is shown in Fig. 1 for the angle $\alpha = \pi/4$ and output coordinates $x_o = y_o = 0$ (see Fig. 1(a)) and $2x_o = y_o = 1$ (see Fig. 1(b)).

Since the GT belongs to the class of the linear integral canonical transforms its kernel is

parametrized by the symplectic 4×4 matrix $\mathbf{T}(\alpha)$ [6, 7]

$$\begin{pmatrix} \mathbf{r}_o \\ \mathbf{q}_o \end{pmatrix} = \begin{bmatrix} \mathbf{X} & \mathbf{Y} \\ -\mathbf{Y} & \mathbf{X} \end{bmatrix} \begin{pmatrix} \mathbf{r}_i \\ \mathbf{q}_i \end{pmatrix} = \mathbf{T}(\alpha) \begin{pmatrix} \mathbf{r}_i \\ \mathbf{q}_i \end{pmatrix},$$

(2)

where

$$\mathbf{X} = \begin{bmatrix} \cos\alpha & 0 \\ 0 & \cos\alpha \end{bmatrix}, \quad \mathbf{Y} = \begin{bmatrix} 0 & \sin\alpha \\ \sin\alpha & 0 \end{bmatrix},$$

(3)

which describes in the paraxial approximation the ray transformation in this system. Notice that $\mathbf{r}^t = (x, y)$ is the ray position and $\mathbf{q}^t = (q_x, q_y)$ is the ray slope, and bold capital here and further indicates matrix notation.

Based on the matrix formalism for first-order lossless optical systems, it has been recently shown [8] that the GT for the large range of angles α can be realized by an optimized flexible optical system which contains only three generalized lenses with fixed distance between them. The angle α is changed by rotation of the cylindrical lenses which form the generalized lenses. Other possibility is to use the spatial light modulator for variable lens performance. Explicit equations for these generalized lenses as a function of the transformation angle α can be found in [8].

2. Basic properties of the gyrator operation

In order to work properly with the GT and to design the corresponding optical system for its experimental realization we need to know its basic properties. As in the case of the Fourier transform (FT) or the fractional FT [9] the main theorems such as scaling, shift, modulation, etc. have to be formulated.

From the equations Eq. (1) - (3) it is easy to see that the GT is periodic and additive with respect to parameter α. The last can be proved directly by the multiplication of the ray transformation matrices which parametrized the kernel: $\mathbf{T}(\alpha)\mathbf{T}(\beta) = \mathbf{T}(\alpha+\beta)$. The inverse GT corresponds to the GT at angle $-\alpha$. As it follows from Eq. (1) the inverse transform can be also written as

$$R^{-\alpha}[f_i(x_i, y_i)](x_o, y_o) = R^{\alpha}[f_i(-x_i, y_i)](-x_o, y_o),$$

(4)

and then $R^{\alpha}\left[R^{\alpha}[f_i(-x_i, y_i)](-x_o, y_o)\right](\mathbf{r}) = f_i(\mathbf{r})$.

It is known that the Parseval relation holds for entire class of the canonical integral transforms and therefore for the gyrator operation which belongs to it. It is easy to demonstrate this relation for the case of the gyrator operation, as it is shown in Eq. (5):

$$\int R^{\alpha}[f_i(\mathbf{r}_i)](\mathbf{r}_o)\left(R^{\alpha}[g_i(\mathbf{r}_e)](\mathbf{r}_o)\right)^* d\mathbf{r}_o = \iint f_i(\mathbf{r}_i) \exp\left(i2\pi \frac{(x_o y_o + x_i y_i)\cos\alpha - (x_i y_o + x_o y_i)}{\sin\alpha}\right) d\mathbf{r}_i$$

$$\times \frac{1}{\sin^2\alpha} \int g_i^*(\mathbf{r}_e) \exp\left(i2\pi \frac{-(x_o y_o + x_e y_e)\cos\alpha + (x_e y_o + x_o y_e)}{\sin\alpha}\right) d\mathbf{r}_e d\mathbf{r}_o$$

$$= \frac{1}{\sin^2\alpha} \int\int f_i(\mathbf{r}_i) g_i^*(\mathbf{r}_e) \exp\left(i2\pi \frac{(x_i y_i - x_e y_e)\cos\alpha}{\sin\alpha}\right)$$

$$\times \int \exp\left(-i2\pi \frac{(x_i - x_e)y_o + x_o(y_i - y_e)}{\sin\alpha}\right) d\mathbf{r}_o d\mathbf{r}_i d\mathbf{r}_e$$

$$= \iint f_i(\mathbf{r}_i) g_i^*(\mathbf{r}_e) \exp\left(i2\pi \frac{(x_i y_i - x_e y_e)\cos\alpha}{\sin\alpha}\right) \delta(\mathbf{r}_i - \mathbf{r}_e) d\mathbf{r}_i d\mathbf{r}_e$$

$$= \int f_i(\mathbf{r}_i) g_i(\mathbf{r}_i)^* d\mathbf{r}_i.$$

(5)

The shift of the function f_i at vector $\mathbf{v}^t = (v_x, v_y)$ leads to the shift of its GT (for the angle α) at $\mathbf{v}\cos\alpha$ and additional linear phase modulation:

$$R^\alpha[f_i(\mathbf{r}_i - \mathbf{v})](\mathbf{r}_o) = \exp\left(i\pi(v_x v_y \sin 2\alpha - 2\mathbf{r}_o^t \tilde{\mathbf{v}} \sin\alpha)\right) R^\alpha[f_i(\mathbf{r}_i)](\mathbf{r}_o - \mathbf{v}\cos\alpha), \qquad (6)$$

where $\tilde{\mathbf{v}}^t = (v_y, v_x)$, see appendix for more details. We observe that the shift of the amplitude of the GT $|R^\alpha[f_i(\mathbf{r}_i - \mathbf{v})](\mathbf{r}_o)| = |R^\alpha[f_i(\mathbf{r}_i)](\mathbf{r}_o - \mathbf{v}\cos\alpha)|$ is the same as for the case of two dimensional symmetric fractional FT at angle α [9].

The effect of plane wave modulation $\exp(-i2\pi\mathbf{k}^t\mathbf{r}_i)$ of the function $f_i(\mathbf{r}_i)$ is also similar to the fractional FT case. It leads to the shift of its GT (for the angle α) at $-\tilde{\mathbf{k}}\sin\alpha$ and additional linear phase modulation:

$$R^\alpha[f_i(\mathbf{r}_i)\exp\left(-i2\pi\mathbf{k}^t\mathbf{r}_i\right)](\mathbf{r}_o) = \exp\left(-i\pi\left(k_x k_y \sin 2\alpha + 2\mathbf{k}^t\mathbf{r}_o\cos\alpha\right)\right) R^\alpha[f_i(\mathbf{r}_i)]\left(\mathbf{r}_o + \tilde{\mathbf{k}}\sin\alpha\right), \tag{7}$$

where $\mathbf{k}^t = (k_x, k_y)$ and $\tilde{\mathbf{k}}^t = (k_y, k_x)$.

Scaling theorem can be formulated in the following form (see appendix section):

$$R^\alpha[f_i(\mathbf{S}\mathbf{r}_i)](\mathbf{r}_o) = \frac{\sigma_\beta \cos\beta}{\sigma_\alpha \cos\alpha} \exp\left(i2\pi x_o y_o \left(1 - \left(\frac{\cos\beta}{\cos\alpha}\right)^2\right)\cot\alpha\right) R^\beta[f_i(\mathbf{r}_i)]\left(\frac{\cos\beta}{\cos\alpha}\mathbf{S}\mathbf{r}_o\right), \tag{8}$$

where $\sigma_\alpha = \mathrm{sgn}(\sin\alpha)$, $\sigma_\beta = \mathrm{sgn}(\sin\beta)$,

$$\mathbf{S} = \begin{pmatrix} s_x & 0 \\ 0 & s_y \end{pmatrix} \quad \text{and} \quad \cot\beta = \frac{\cot\alpha}{s_x s_y}. \tag{9}$$

It means that the GT at angle α of the scaled function $f_i(\mathbf{S}\mathbf{r}_i)$ corresponds to the GT at angle β of the initial function $f_i(\mathbf{r}_i)$ with additional scaling of the output coordinates and hyperbolic phase modulation. The scaling property for the GT is similar to one for the Fresnel transform or for the symmetrical fractional FT. Indeed during the Fresnel diffraction the change of the aperture scale leads to the observation of the same diffraction pattern (except of the corresponding scaling and chirp phase modulation) at another propagation distance. The principal difference is in the phase modulation which has hyperbolic form for the GT and chirp form for Fresnel or fractional FT transforms. Moreover in the case of GT there are two particular cases of scaling parameters $s_x = s = s_y^{-1}$ and $s_x = s = -s_y^{-1}$ when the expression Eq. (8) is significantly reduced.

Thus if $s_x = s = s_y^{-1}$ the scaling does not change the transformation angle $\beta = \alpha$, the output scaling is the same as the input one and there is no additional phase modulation

$$R^\alpha[f_i(x_i s, y_i s^{-1})](\mathbf{r}_o) = R^\alpha[f_i(\mathbf{r}_i)](x_o s, y_o s^{-1}). \tag{10}$$

This scaling property will be demonstrated in section 4.1 in application to generation of elliptical vortex beams.

If $s_x = s = -s_y^{-1}$ then the angles relation reduces to $\cot\beta = -\cot\alpha$ and therefore $\beta = \pi - \alpha$. The Eq. (8) can be written as

$$R^\alpha[f_i(x_i s, -y_i s^{-1})](\mathbf{r}_o) = R^{\pi-\alpha}[f_i(\mathbf{r}_i)]\left(-x_o s, s^{-1} y_o\right), \tag{11}$$

or using the additive property of the GT as

$$R^\alpha[f_i(x_i s, -y_i s^{-1})](\mathbf{r}_o) = R^{-\alpha}[f_i(\mathbf{r}_i)]\left(x_o s, -s^{-1} y_o\right). \tag{12}$$

In particular for $s = 1$ we obtain the expression similar to Eq. (4).

$$R^\alpha[f_i(x_i, -y_i)](\mathbf{r}_o) = R^{-\alpha}[f_i(\mathbf{r}_i)](x_o, -y_o). \tag{13}$$

3. Gyrator transform of selected functions

As it occurs for the Fourier transform the GT of only selected functions can be expressed analytically. The fundamental functions: Dirac delta, 1, hyperbolic wave, plane wave, spherical wave, Gaussian and Hermite-Gaussian mode and their GTs are displayed in Table 1. The following notations are used along the Table: $\mathbf{v}^t = (v_x, v_y)$, $\mathbf{k}^t = 2\pi(k_x, k_y)$, $a > 0$, b and c are real numbers, and $\Re^{-\frac{\pi}{4}}$ is the operator of coordinate rotation at angle $-\pi/4$.

Table 1. Selected functions and their gyrator transforms

$f_i(\mathbf{r}_i)$	$f_o(\mathbf{r}_o) = R^\alpha[f_i(\mathbf{r}_i)](\mathbf{r}_o)$
$\delta(\mathbf{r}_i - \mathbf{v})$	$\frac{1}{\lvert\sin\alpha\rvert}\exp\left(i2\pi\frac{(x_oy_o+v_xv_y)\cos\alpha-(v_xy_o+x_ov_y)}{\sin\alpha}\right)$
$\exp(i2\pi cx_iy_i)$	$\frac{1}{\lvert\sin\alpha\rvert}\exp\left(i2\pi\frac{c\cot\alpha-1}{c+\cot\alpha}x_oy_o\right),\ (c \neq -\cot\alpha)$
1	$\frac{1}{\lvert\sin\alpha\rvert}\exp(-i2\pi x_oy_o\tan\alpha)$
$\exp(-i\mathbf{k}^t\mathbf{r}_i)$	$\frac{1}{\lvert\sin\alpha\rvert}\exp(-i2\pi(x_oy_o+k_xk_y)\tan\alpha)\exp\left(-\frac{i}{\cos\alpha}\mathbf{k}^t\mathbf{r}_o\right)$
$\exp(-i\pi b\mathbf{r}_i^2)$	$\frac{1}{\sqrt{\cos^2\alpha-b^2\sin^2\alpha}}\exp\left(-i\pi\frac{(1+b^2)\sin 2\alpha}{\cos^2\alpha-b^2\sin^2\alpha}x_oy_o\right)\exp\left(\frac{-i\pi b\mathbf{r}_o^2}{\cos^2\alpha-b^2\sin^2\alpha}\right)$
$\exp(-\pi a\mathbf{r}_i^2)$	$\frac{1}{\sqrt{\cos^2\alpha+a^2\sin^2\alpha}}\exp\left(i\pi\frac{(a^2-1)\sin 2\alpha}{\cos^2\alpha+a^2\sin^2\alpha}x_oy_o\right)\exp\left(\frac{-\pi a\mathbf{r}_o^2}{\cos^2\alpha+a^2\sin^2\alpha}\right)$
$HG_{m,n}\left(\Re^{-\frac{\pi}{4}}\mathbf{r}_i;1\right)$	$e^{i\alpha(n-m)}HG_{m,n}\left(\Re^{-\frac{\pi}{4}}\mathbf{r}_o;1\right)$

Let us consider in detail some particular cases from Table 1 (see appendix for intermediate calculation). The first row of Table 1 shows that the GT for $\delta(\mathbf{r}_i - \mathbf{v})$ corresponds to the gyrator kernel as the output function, $K_\alpha(\mathbf{r}_i = \mathbf{v}, \mathbf{r}_o)$, and therefore the product of hyperbolic and plane waves.

Correspondingly the GT of a hyperbolic wave (see row 2, Table 1) transforms to Dirac function for angle such that $\cot\alpha = -c$. It is an important result because it means that GT can be used for localization of waves with hyperbolic phase front. For $c = \tan\alpha$ the plane wavefront, $f_o(\mathbf{r}_o) = \lvert\sin\alpha\rvert^{-1}$, is obtained at the output of the GT system. For other angles the hyperbolic wave transforms to the hyperbolic one. We underline only two particular cases, when the expressions for the GT of hyperbolic wave are simplified. Thus for the values of parameter $c = \cot\alpha$ and $c = (1+\cot\alpha)/(\cot\alpha-1)$ we obtain $f_o(\mathbf{r}_o) = \exp(i\pi(\cot\alpha-\tan\alpha)x_oy_o)/\lvert\sin\alpha\rvert$ and $f_o(\mathbf{r}_o) = \exp(i2\pi x_oy_o)/\lvert\sin\alpha\rvert$ respectively. Note that for $c = 0$ ($f_i(\mathbf{r}_i) = 1$) the GT also corresponds to a hyperbolic wavefront as it is indicated at the third row of the Table 1.

The gyrator transform of a plane wave (row 4, Table1) corresponds to a product of the plane wave, with spatial frequency scaled by $1/\cos\alpha$ and the hyperbolic wave.

For the spherical wavefront (row 5, Table 1) its GT corresponds to a product of the spherical wave, affected by the scaling factor and the hyperbolic wave. The hyperbolic contribution cancels for angles corresponding to position and rotated FT domains $\alpha = \pi(2n+1)/2$ ($f_o(\mathbf{r}_o) = \exp(i\pi\mathbf{r}_o^2/b)/ib$) and $\alpha = \pi n$ ($f_o(\mathbf{r}_o) = \exp(-i\pi b\mathbf{r}_o^2)$), where n is an integer.

The GT of a Gaussian function (row 6, Table 1) corresponds to the Gaussian function with hyperbolic phase modulation. In the case $a = 1$ the additional phase shift vanishes and output function corresponds to the input function $\exp(-\pi r_o^2)$. This result indicates that $\exp(-\pi r_o^2)$ is an eigenfunction of the GT for any transformation angle α.

It has been shown in [10] that the GT at angle α can be represented as a fractional separable Fourier transform at angles $(\alpha, -\alpha)$ with rotation of the input and output coordinates (x, y) at $\pi/4$ and $-\pi/4$ correspondingly. From that follows (see reference [11]) that the eigenfunctions for the GT are the eigenfunctions of the fractional FT rotated at angle $-\pi/4$. Since the Hermite Gaussian modes:

$$HG_{m,n}(\mathbf{r};w) = 2^{1/2} \frac{H_m\left(\sqrt{2\pi}\frac{x}{w}\right) H_n\left(\sqrt{2\pi}\frac{y}{w}\right)}{\sqrt{2^m m! w}\sqrt{2^n n! w}} \exp\left(-\frac{\pi}{w^2}\mathbf{r}^2\right), \tag{14}$$

where H_m is the Hermite polynomial and w is the beam waist, form the complete orthogonal set of eigenfunctions for the separable fractional FT for $w = 1$ then the HG modes rotated at $-\pi/4$ form the set of the orthogonal eigenfunctions for the GT (row 7, Table 1).

For $\alpha = \pm\pi/4$ the kernel of the GT is reduced to

$$K_{\pm\pi/4}(x_i, y_i, x_o, y_o) = \sqrt{2}\exp\left(\pm i2\pi\left[x_o y_o + x_i y_i - \sqrt{2}\left(x_i y_o + x_o y_i\right)\right]\right). \tag{15}$$

In this case as it was shown (for example in [3, 4]) that the $HG_{m,n}(\mathbf{r};w)$ for $w = 1$ mode transforms into the helicoidal LG mode:

$$LG_{p,l}^{\pm}(\mathbf{r};w) = w^{-1}\sqrt{\frac{\min(m,n)!}{\max(m,n)!}}\left(\sqrt{2\pi}\left(\frac{x}{w} \pm i\frac{y}{w}\right)\right)^l L_p^l\left(\frac{2\pi}{w^2}\mathbf{r}^2\right)\exp\left(-\frac{\pi}{w^2}\mathbf{r}^2\right), \tag{16}$$

where L_p^l is the Laguerre polynomial, $p = \min(m,n)$ and $l = |m - n|$. The topological charge of the vortex mode is given by $\pm l$.

For the transformation angle $\alpha = 3\pi/4$, $5\pi/4$ as it follows from Eq. (4) and Eq. (11) $HG_{m,n}(\mathbf{r};1)$ mode transforms to $-LG_{p,l}^{-}(\mathbf{r};1)$ and $-LG_{p,l}^{+}(\mathbf{r};1)$, respectively.

Finally we consider the GT of periodic functions. It is well-known that a periodic function $f_i(\mathbf{r}_i)$ with periods k_x^{-1}, k_y^{-1} can be written as a Fourier expansion

$$f_i(\mathbf{r}_i) = \sum_{n,m} a_{n,m}\exp\left(-i2\pi\left(x_i k_x n + y_i k_y m\right)\right). \tag{17}$$

Then the GT of a periodic function is given by

$$f_o(\mathbf{r}_o) = R^\alpha[f_i(\mathbf{r}_i)](\mathbf{r}_o) = \sum_{n,m} a_{n,m} R^\alpha[\exp\left(-i2\pi\left(x_i k_x n + y_i k_y m\right)\right)](\mathbf{r}_o). \tag{18}$$

Using the expression for the GT of a plane wave (row 4, Table 1) we derive that

$$f_o(\mathbf{r}_o) = \frac{\exp\left(-i2\pi x_o y_o \tan\alpha\right)}{|\sin\alpha|}\sum_{n,m} a_{n,m}\exp\left(-i2\pi nmk_x k_y \tan\alpha\right)\exp\left(-i2\pi\frac{nk_x x_o + mk_y y_o}{\cos\alpha}\right). \tag{19}$$

An interesting result is obtained for angles which satisfy the relation $l = k_x k_y \tan\alpha_l$, where l is an integer. Then Eq. (19) is reduced to

$$f_o(\mathbf{r}_o) = \frac{\exp\left(-i2\pi x_o y_o \tan\alpha_l\right)}{|\sin\alpha_l|} f_i\left(\frac{1}{\cos\alpha_l}\mathbf{r}_o\right), \tag{20}$$

which can be considered as a Talbot effect for the gyrator transform.

Finally as an example, figure 2 shows the squared moduli (intensity distribution in the case of optical realization) of the GT for the circle function $circ(r_i/\rho)$ ($\rho = 1.6$) for different transformation angles $\alpha = 0$, $7\pi/36$, $\pi/4$, $11\pi/36$, $\pi/2$, (a-e) respectively. This image sequence Fig. 2(a-e) demonstrates the evolution from the input function Fig. 2(a) to its rotated Fourier transform obtained for $\alpha = \pi/2$, Fig. 2(e). We observe how the rotational symmetry in the position ($\alpha = 0$) and FT domain ($\alpha = \pi/2$) changes to the rectangular one for other angles.
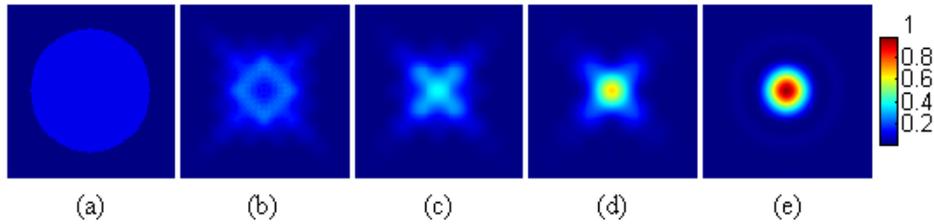
Fig. 2. Intensity distributions corresponding to the GT of the circle function are displayed for different transformation angles $\alpha = 0$ (a),$7\pi/36$ (b), $\pi/4$ (c), $11\pi/36$ (d), and $\pi/2$ (e). Note that for $\alpha = \pi/2$ the rotated Fourier transform is obtained.

4. Gyrator transform applications

The above mentioned properties of the GT make it a useful tool for optical information processing. The GT provides an image representation in a new phase-space domain which was not explored yet for signal analysis and synthesis. In particular it can be used for hyperbolic wave detection, shift-variant filtering, encryption, beam characterization, generation of stable modes with specific properties. The application of the GT for all these tasks certainly demands extensive studies. Here we will consider only the mode transformation under the GT. In particular we will consider the gyrator transformation of the Hermite-Gaussian modes. There is a double interest to these modes. First of all they appear as a natural modes in laser resonators of rectangular symmetry and propagate in a free space without changing their intensity form. On the other hand the HG modes forms a complete orthonormal set and therefore often are used as a basis for image representation. The GT of the HG modes generates other stable modes, which also propagate in free space without changing their intensity form and the knowledge of these modes permits to represent any image in the corresponding GT domain.

4.1. Hermite-Gaussian mode evolution under the gyrator transform

Let us consider the evolution oh the HG mode (14) under the GT. Since the GT for different angles can be performed by optical system constructed from three generalized lenses (assembled set of cylindrical lenses) and two fixed free space intervals [8] the numerical simulations of the GT can follow this recipe. Using free space propagation algorithm under Fresnel diffraction regime and phase modulation functions for the generalized lenses we calculated the output patterns for the GT system. The parameters used in these numerical simulations are the following: wavelength $\lambda = 532nm$, $w = 0.73mm$, and spatial resolution $20\mu m$.

During last decade various optical schemes were proposed for the generation of the vortex beams which carry the orbital angular momentum (OAM). Mostly the conversion of Hermite-Gaussian ($HG_{m,n}$) modes of different orders to the helicoidal Laguerre-Gaussian ($LG_{p,l}$) ones were considered [2]. It was also shown that it is possible to generate the stable modes with fractional orbital angular momentum [4, 5]. The GT can be seen as a flexible mode converter where modes of the same order but different OAM are obtained by varying the angle α. As it was indicated in the previous section the mode conversion from $HG_{m,n}$ to $LG_{p,l}$, and viceversa, is achieved when $\alpha = \pi/4 + n\pi/2$ (n integer), meanwhile other modes are obtained for the rest of angle values if $\alpha \neq \pi n/2$.
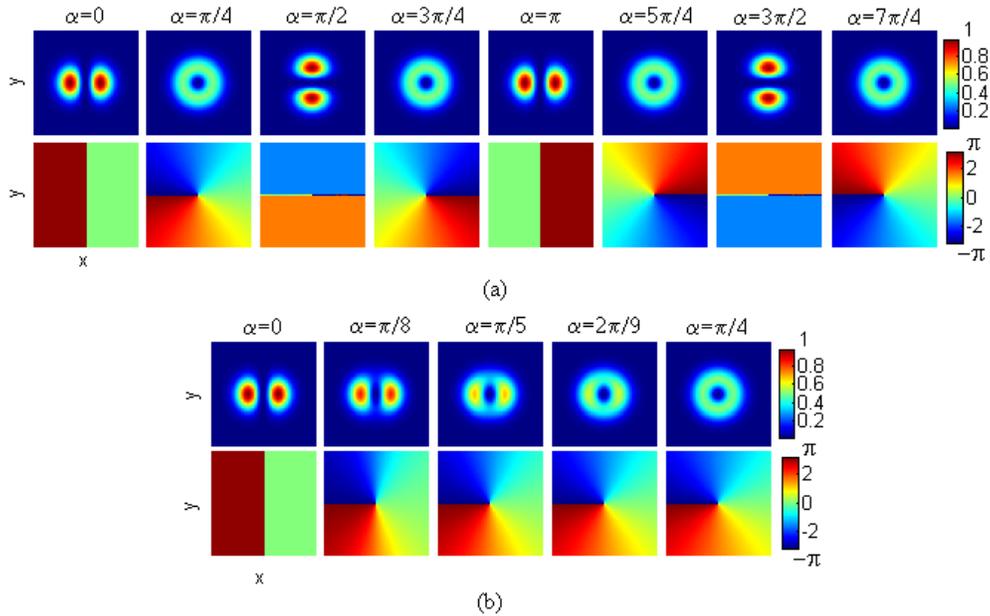
Fig. 3. Intensity (up row) and phase (low row) of the GT of $HG_{1,0}$ mode for different angles α. Figure (a) corresponds to transformation angle $\alpha = 0$, $\pi/4$, $\pi/2$, $3\pi/4$, π, $5\pi/4, 3\pi/2, 7\pi/4$. (b) Intermediate sequence between angle $\alpha = 0$ and $\alpha = \pi/4$ is displayed. (2.5 MB) Movie: mode transformation for different angles α, where the input mode is $HG_{1,0}$.

In Figure 3 the mode conversion from $HG_{m,n}$ mode of order $m = 1$, $n = 0$ to helicoidal $LG_{p=0,l=1}$ is displayed for different values of angle α. The first and the second rows correspond to the intensity and phase distribution, respectively. The intensity distribution is normalized to the maximum intensity value of the input signal ($\alpha = 0$), and phase values are represented for $[-\pi, \pi]$ region. Mode conversion from $HG_{1,0}$ ($\alpha = 0$) to $LG_{0,1}^{\pm}$ is obtained for $\alpha = \pi/4$, $3\pi/4$, $5\pi/4, 7\pi/4$, as it has been explained in Section 3. For $\alpha = \pi/2$, π, $3\pi/2$ the output mode corresponds to $HG_{1,0}$ rotated at $\pi/2$, $\pi, 3\pi/2$ with additional phase shift $\exp(i2\alpha)$, respectively. Therefore the mode conversion from $HG_{1,0}$ to $HG_{0,1}$ is obtained for $\alpha = \pi/2$, $3\pi/2$. In Fig. 3(b) the intermediate modes obtained by the GT of $HG_{1,0}$ for $\alpha = [0, \pi/4]$ are displayed. The modes obtained for every particular angle α are stable and possess fractional OAM [5]. In general the action of the GT is associated with the movement along the main meridian of the Poincaré spheres.

4.2. Influence of scaling and shift properties to mode transformation

Let us now consider how the scaling of the input HG mode affects on the mode generation. Based on the scaling theorem (8) and choosing scaling parameters $s_x = s = s_y^{-1}$ in order to avoid the change of the transformation angle and additional phase modulation, we observe (see Fig. 4) that for $\alpha = \pi/4$ the transformation of the rotational symmetric intensity distribution typical for the LG mode into elliptical one (Fig. 4c, Fig. 4f). Figures 4 (a) and (d) correspond to the input signal $HG_{1,0}$ scaled by $s = 1/2$ and $s = 2$, respectively. Figures 4 (b, c) and (e, f) are the corresponding output modes for $\alpha = \pi/5$ and $\alpha = \pi/4$. Therefore the GT of scaled HG mode is an alternative for generation of the elliptic LG beams [14].
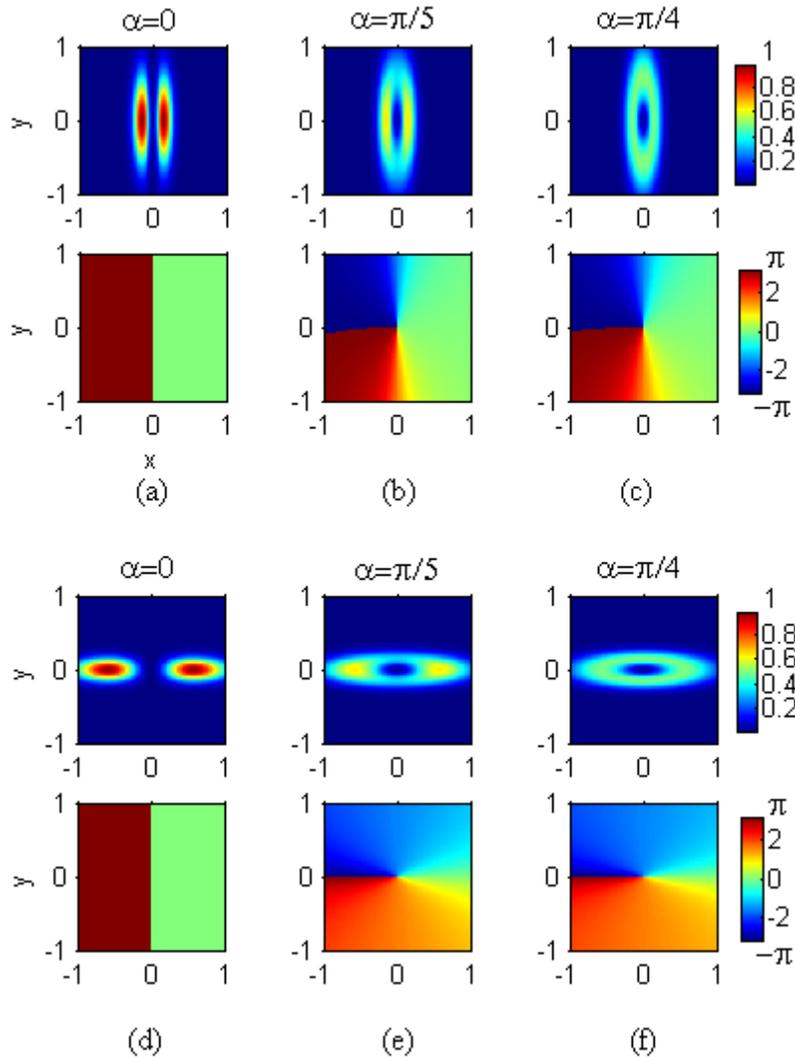
Fig. 4. Intensity (up row) and phase (low row) for different angles of the GT of $HG_{1,0}$ affected by scaling factors $s_x = s = s_y^{-1}$: $s = 1/2$ (a, b, c) and $s = 2$ (d, e ,f), respectively.

When the input function is not centred at the optical axis we can apply the shifting theorem, Eq. (6), to obtain the output function. Notice that if the input signal is shifted at $\mathbf{v}^t = (v_x, v_y)$ the output signal is shifted at $\mathbf{v}^t \cos\alpha$ and affected by an additional linear phase modulation. The GT at angle $\alpha = \pi/5$ and $\alpha = \pi/4$ of $HG_{1,0}$ for different shifting parameters is displayed in Fig. 5. Figures 5 (b, c) and (e, f) are the output modes obtained from the $HG_{1,0}$ mode shifted by $\mathbf{v}^t = (1mm, 0)$ (Fig. 5a) and $\mathbf{v}^t = (1mm, -1mm)$ (Fig. 5c), respectively.

4.3. Gyrator transform of HG mode composition

Up till now we have considered the transformation of only one HG mode. Nevertheless the composition of HG modes of the same order ($n + m = const$) also produces a stable configuration after gyrator transformation. Thus for example the combination of $HG_{3,0}$ and $HG_{0,3}$ modes:
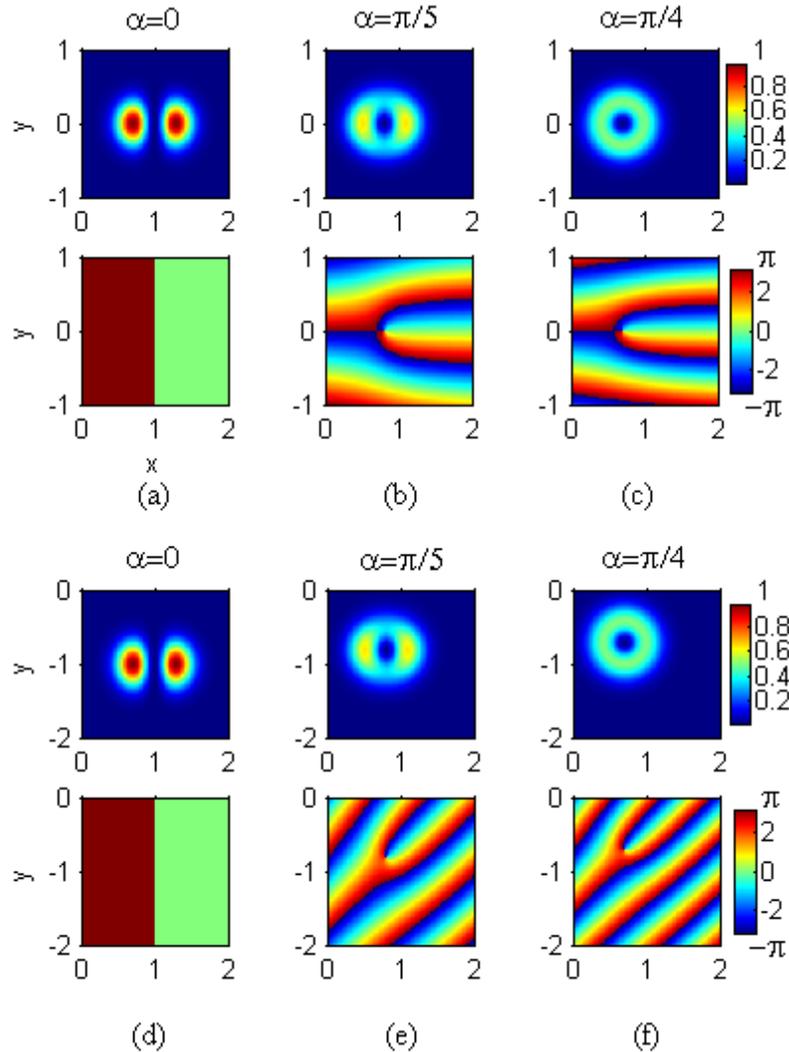
Fig. 5. Intensity (up row) and phase (low row) of the GT (for the angle α) of $HG_{1,0}$ mode shifted by $\mathbf{v}^t = (1mm, 0)$ (a, b, c) and $\mathbf{v}^t = (1mm, -1mm)$ (d, e, f).

$HG_{3,0} + HG_{0,3}$ (Fig. 6a) leads for $\alpha = \pi/4$ to the odd Laguerre-Gaussian beams, which is the sum of two helicoidal LG modes with opposite OAM values: $LG_{0,3}^+ + LG_{0,3}^-$ (Fig. 6e). For other angles $\alpha = \pi/8$, $\pi/5$, $2\pi/9$ the intermediate modes are obtained (Fig. 6 b, c, d).

5. Conclusion

A little known operation for two-dimensional signal manipulation, called gyrator transform, has been studied. The main properties of the GT such as shift, scaling, plane wave modulation, Parseval theorem, and other relevant properties have been formulated. The GTs of the selected functions have been also found. The gyrator operation promises to be a useful tool in image processing, holography, beam characterization, quantum information, new mode generation, etc. For example, here it has been demonstrated its application for stable mode generator. The
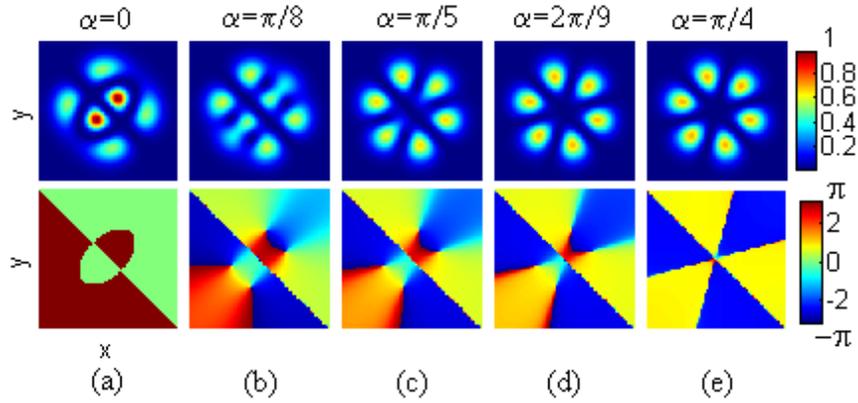
Fig. 6. Intensity (up row) and phase (low row) distributions for GT of the $HG_{3,0} + HG_{0,3}$ input mode are displayed for different angles $\alpha = 0$ (input mode), $\pi/8$, $\pi/5$, $2\pi/9$, $\pi/4$ ($LG_{0,3}^+ + LG_{0,3}^-$ mode). (2.8 MB) Movie: mode transformation for different angles α, where the input mode is $HG_{3,0} + HG_{0,3}$.

experimental scheme for optical implementation of the GT has been recently constructed by the authors. The preliminary results, not displayed in this paper, demonstrate very good agreement with theoretical predictions which opens new perspectives for different applications.

Acknowledgements

Appendix

In this appendix we demonstrate the shift and scaling theorems associated to the gyrator transformation and present the main intermediate calculations for the GT of the selected functions from the Table 1, which were discussed previously.

Shift theorem for gyrator transform

The kernel of the GT (Eq. (1)) is parametrized by the symplectic matrix $\mathbf{T}(\alpha)$ as we have mentioned previously, Eq. (2) and (3). Therefore the Eq. (1) can be rewritten as follows:

$$f_o(\mathbf{r}_o) = R^\alpha[f_i(\mathbf{r}_i)](\mathbf{r}_o) = \frac{1}{|\sin\alpha|} \iint f_i(\mathbf{r}_i) \exp\left(i\pi\left(\mathbf{r}_i^t\mathbf{Y}^{-1}\mathbf{X}\mathbf{r}_i - 2\mathbf{r}_i^t\mathbf{Y}^{-1}\mathbf{r}_o + \mathbf{r}_o^t\mathbf{X}\mathbf{Y}^{-1}\mathbf{r}_o\right)\right) d\mathbf{r}_i. \tag{21}$$

Here t stands for transposition operation. In order to demonstrate the shift theorem it is suitable to apply this equation (21). Considering that the input function is affected by a shift which is indicated by means of the vector $\mathbf{v}^t = (v_x, v_y)$, where $\mathbf{u} = \mathbf{r}_i - \mathbf{v}$, we derive

$$f_o(\mathbf{r}_o) = \frac{1}{|\sin\alpha|} \iint f_i(\mathbf{r}_i - \mathbf{v}) \exp\left(i\pi\left(\mathbf{r}_i^t\mathbf{Y}^{-1}\mathbf{X}\mathbf{r}_i - 2\mathbf{r}_i^t\mathbf{Y}^{-1}\mathbf{r}_o + \mathbf{r}_o^t\mathbf{X}\mathbf{Y}^{-1}\mathbf{r}_o\right)\right) d\mathbf{r}_i$$

$$= \frac{1}{|\sin\alpha|} \iint f_i(\mathbf{u}) \exp\left(i\pi\left((\mathbf{u}+\mathbf{v})^t\mathbf{Y}^{-1}\mathbf{X}(\mathbf{u}+\mathbf{v}) - 2(\mathbf{u}+\mathbf{v})^t\mathbf{Y}^{-1}\mathbf{r}_o + \mathbf{r}_o^t\mathbf{X}\mathbf{Y}^{-1}\mathbf{r}_o\right)\right) d\mathbf{u}$$

$$= \frac{1}{|\sin\alpha|} \iint f_i(\mathbf{u}) \exp\left(i\pi\phi\right) d\mathbf{u}. \tag{22}$$

The kernel $\exp(i\pi\phi)$ is simplified as

$$
\begin{aligned}
\exp(i\pi\phi) = \exp\big(i\pi(\mathbf{v}^t\mathbf{Y}\mathbf{X}\mathbf{v}+\mathbf{r}_o^t[(\mathbf{X}\mathbf{Y}^{-1}\mathbf{X}-(\mathbf{Y}^{-1})^t-\mathbf{Y}]\mathbf{v}))\times \\
\exp\big(i\pi\left(\mathbf{r}_i^t\mathbf{Y}^{-1}\mathbf{X}\mathbf{r}_i-2\mathbf{r}_i^t\mathbf{Y}^{-1}\left(\mathbf{r}_o-\mathbf{X}\mathbf{v}\right)+\left(\mathbf{r}_o-\mathbf{X}\mathbf{v}\right)^t\mathbf{X}\mathbf{Y}^{-1}\left(\mathbf{r}_o-\mathbf{X}\mathbf{v}\right)\right)\big),
\end{aligned}
\tag{23}
$$

where the following relations ($\mathbf{I}$ is a unity 2×2 matrix) have been used

$$
\begin{aligned}
\mathbf{v}^t\mathbf{Y}^{-1}\mathbf{X}\mathbf{u} &= \mathbf{u}^t\left(\mathbf{Y}^{-1}\mathbf{X}\right)^t\mathbf{v} = \mathbf{u}^t\mathbf{X}^t\left(\mathbf{Y}^{-1}\right)^t\mathbf{v}, \\
\mathbf{X}\mathbf{Y}^t &= \mathbf{Y}\mathbf{X}^t, \\
\mathbf{X}^t\mathbf{X}+\mathbf{Y}^t\mathbf{Y} &= \mathbf{I}.
\end{aligned}
\tag{24}
$$

The equation (23) has two exponential functions. The first one corresponds to an additional phase factor that can be extracted from the integral in Eq. (22), and the second one corresponds to the gyrator kernel where the coordinate $\mathbf{r}_o$ is replaced by $\mathbf{r}_o-\mathbf{X}\mathbf{v}$. Doing this we obtain the shift theorem as it was formulated in (6)

$$
\begin{aligned}
f_o(\mathbf{r}_o) &= R^\alpha[f_i(\mathbf{r}_i-\mathbf{v})](\mathbf{r}_o) \\
&= \exp\big(i\pi(\mathbf{v}^t\mathbf{Y}\mathbf{X}\mathbf{v}+\mathbf{r}_o^t[(\mathbf{X}\mathbf{Y}^{-1}\mathbf{X}-(\mathbf{Y}^{-1})^t-\mathbf{Y}]\mathbf{v})\big)R^\alpha[f_i(\mathbf{r}_i)](\mathbf{r}_o-\mathbf{X}\mathbf{v}) \\
&= \exp\big(i\pi(v_xv_y\sin2\alpha-2\mathbf{r}_o\widetilde{\mathbf{v}}\sin\alpha)\big)R^\alpha[f_i(\mathbf{r}_i)](\mathbf{r}_o-\mathbf{v}\cos\alpha),
\end{aligned}
\tag{25}
$$

where $\widetilde{\mathbf{v}}=(v_y,v_x)$. Finally, it is demonstrated that the shift of the function f_i at vector $\mathbf{v}^t=(v_x,v_y)$ leads to the shift of its GT (for the angle α) at $\mathbf{v}\cos\alpha$ and additional linear phase modulation.

Scaling theorem for gyrator transform

For the case of the scaling theorem the input function is affected by a scaling factor $f_i(\mathbf{S}\mathbf{r}_i)=f_i(s_xx_i,s_yy_i)$. Therefore applying a change of variable $x_i'=s_xx_i$, $y_i'=s_yy_i$ for the equation Eq. (1), we obtain:

$$
\begin{aligned}
f_o(\mathbf{r}_o) &= R^\alpha[f_i(\mathbf{S}\mathbf{r}_i)](\mathbf{r}_o) \\
&= \frac{\exp(i2\pi x_oy_o\cot\alpha)}{s_xs_y|\sin\alpha|}\iint f_i(x_i',y_i')\exp\left(i2\pi\left(x_i'y_i'\frac{\cot\alpha}{s_xs_y}-\frac{1}{\sin\alpha}\left(\frac{x_i'y_o}{s_x}+\frac{x_oy_i'}{s_y}\right)\right)\right)dx_i'dy_i'.
\end{aligned}
\tag{26}
$$

The next step is to define $\cot\beta=\cot(\alpha)/s_xs_y$, then the last equation is rewritten as follows:

$$
\begin{aligned}
f_o(\mathbf{r}_o) &= \frac{\exp(i2\pi x_oy_o\cot\alpha)}{s_xs_y|\sin\alpha|}\iint f_i(x_i',y_i')\exp\left(i2\pi\left(x_i'y_i'\cot\beta-\frac{1}{\sin\alpha}\left(\frac{x_i'y_o}{s_x}+\frac{x_oy_i'}{s_y}\right)\right)\right)dx_i'dy_i' \\
&= \frac{\exp(i2\pi x_oy_o\cot\alpha)|\sin\beta|}{s_xs_y|\sin\alpha|}\exp\left(-i2\pi\cot\beta\frac{y_ox_o\sin^2\beta}{s_xs_y\sin^2\alpha}\right)R^\beta[f_i(\mathbf{r}_i)]\left(\frac{x_o\sin\beta}{s_y\sin\alpha},\frac{y_o\sin\beta}{s_x\sin\alpha}\right) \\
&= \frac{\sigma_\beta\cos\beta}{\sigma_\alpha\cos\alpha}\exp\left(i2\pi x_oy_o\cot\alpha\left(1-\left(\frac{\cos\beta}{\cos\alpha}\right)^2\right)\right)R^\beta[f_i(\mathbf{r}_i)]\left(\frac{\cos\beta}{\cos\alpha}\mathbf{S}\mathbf{r}_i\right),
\end{aligned}
\tag{27}
$$

where $\sigma_\alpha=\mathrm{sgn}(\sin\alpha)$, $\sigma_\beta=\mathrm{sgn}(\sin\beta)$. In order to obtain this equation the definition of the GT and simple trigonometric relations have been used. We conclude that the GT at angle α of a scaled input function $f_i(\mathbf{S}\mathbf{r}_i)$, corresponds to the GT at angle β of the initial function $f_i(\mathbf{r}_i)$ with additional scaling of the output coordinates and affected by a hyperbolic phase modulation.

Gyrator transform of selected functions, Table 1

Here we present the main intermediates calculations for the GT of the functions from Table 1.

The GT of the Dirac delta function (row 1, Table 1) is obtained directly applying the properties of the δ-function.

The GT of hyperbolic wavefront (row 2, Table 1) and the constant function 1 in particular ($c = 0$) (row 3, Table 1) is calculated as follows:

$$
\begin{aligned}
f_o(\mathbf{r}_o) &= R^\alpha [\exp(i2\pi c x_i y_i)](\mathbf{r}_o) \\
&= \frac{\exp(i2\pi x_o y_o \cot\alpha)}{|\sin\alpha|} \iint \exp\left(i2\pi\left(x_i y_i(c+\cot\alpha) - \frac{1}{\sin\alpha}(x_i y_o + x_o y_i)\right)\right) dx_i dy_i \\
&= \frac{\exp(i2\pi x_o y_o \cot\alpha)}{|\sin\alpha|} \int \exp\left(-i2\pi\frac{x_o y_i}{\sin\alpha}\right) dy_i \int \exp\left(i2\pi x_i \left(y_i(c+\cot\alpha) - \frac{y_o}{\sin\alpha}\right)\right) dx_i \\
&= \frac{\exp(i2\pi x_o y_o \cot\alpha)}{|\sin\alpha|} \int \exp\left(-i2\pi\frac{x_o y_i}{\sin\alpha}\right) \delta\left(y_i(c+\cot\alpha) - \frac{y_o}{\sin\alpha}\right) dy_i \\
&= \frac{\exp(i2\pi x_o y_o \cot\alpha)}{|\sin\alpha|} \exp\left(-i2\pi\frac{x_o y_o}{(c+\cot\alpha)\sin^2\alpha}\right),
\end{aligned}
\tag{28}
$$

where we used that

$$
\delta(v) = \int \exp(i2\pi v x)\, dx.
\tag{29}
$$

The last expression, Eq. (28), is simplified using the trigonometric relations

$$
R^\alpha[\exp(i2\pi c x_i y_i)](\mathbf{r}_o) = \frac{1}{|\sin\alpha|}\exp\left(i2\pi\frac{c\cot\alpha - 1}{c+\cot\alpha}x_o y_o\right).
\tag{30}
$$

A simple change of variable: $x'_o = x_o + k_y \sin\alpha$, and $y'_o = y_o + k_x \sin\alpha$ and the Eq. (29) allow to calculate the GT of a plane wave (row 4, Table 1).

The next two functions correspond to a spherical wavefront and a Gaussian function, (row 5 and 6 Table 1, respectively) and can be derived as particular cases of the GT of function $f_i(\mathbf{r}_i) = \exp(\gamma \mathbf{r}_i^2)$, where $\gamma = -\pi(a+ib)$ and $a \geq 0$. According to Eq. (1) the GT of $f_i(\mathbf{r}_i) = \exp(\gamma \mathbf{r}_i^2)$ is given by

$$
f_o(x_o, y_o) = \frac{1}{|\sin\alpha|}\exp(i2\pi x_o y_o \cot\alpha)\, g_o(x_o, y_o),
\tag{31}
$$

where

$$
\begin{aligned}
g_o(x_o, y_o) &= \iint \exp(\gamma \mathbf{r}_i^2) \exp\left(i2\pi\left(x_i y_i \cot\alpha - \frac{1}{\sin\alpha}(x_i y_o + x_o y_i)\right)\right) dx_i dy_i \\
&= \int \exp(x_i^2 \gamma) \exp\left(-i2\pi\frac{x_i y_o}{\sin\alpha}\right) dx_i \int \exp(y_i^2 \gamma) \exp\left(i2\pi\left(x_i \cot\alpha - \frac{x_o}{\sin\alpha}\right)y_i\right) dy_i \\
&= \sqrt{\frac{\pi}{-\gamma}} \int \exp(x_i^2 \gamma) \exp\left(\frac{\pi^2}{\gamma}\left(x_i \cot\alpha - \frac{x_o}{\sin\alpha}\right)^2\right) \exp\left(-i2\pi\frac{x_i y_o}{\sin\alpha}\right) dx_i.
\end{aligned}
\tag{32}
$$

The last expression in Eq. (32) has been obtained using the following equation

$$
\int \exp(\mu x^2 + \beta x)\, dx = \sqrt{\frac{\pi}{-\mu}}\exp\left(-\frac{\beta^2}{4\mu}\right),
\tag{33}
$$

where $\text{Re}(\mu) \leq 0$, for calculation the integral with respect to y_i. Therefore $\text{Re}(\gamma) \leq 0$ must be satisfied. Using a change of variable $t = x_i\sqrt{\gamma}$, we again apply the Eq. (33) for integration with

respect to x_i and derive that

$$g_o(x_o, y_o) = \sqrt{\frac{\pi^2}{\gamma^2 d}} \exp\left(\frac{\pi^2}{\gamma d \sin^2\alpha}\left(x_o^2 + y_o^2\right)\right) \exp\left(-i2\pi\frac{\pi^2}{d\gamma^2\sin^2\alpha}x_o y_o \cot\alpha\right), \quad (34)$$

where $d = 1 + \left(\pi\cot(\alpha)/\gamma\right)^2$. Then the GT of $f_i(\mathbf{r}_i) = \exp\left(\gamma\mathbf{r}_i^2\right)$ is given by

$$f_o(\mathbf{r}_o) = \frac{\exp\left(i2\pi\left(1 - \frac{1}{\cos^2\alpha + (\gamma/\pi)^2\sin^2\alpha}\right)x_o y_o \cot\alpha\right)}{\sqrt{\cos^2\alpha + (\gamma/\pi)^2\sin^2\alpha}}\exp\left(\frac{\gamma\mathbf{r}_o^2}{\cos^2\alpha + (\gamma/\pi)^2\sin^2\alpha}\right). \quad (35)$$

Finally the GT of the spherical wave and Gaussian function (row 5 and 6 of the Table 1) are obtained from Eq. (35) for $\gamma = -\pi a$ and $\gamma = -i\pi b$, respectively.